International Journal of Pharmaceutics 434 (2012) 334–348

Contents lists available at SciVerse ScienceDirect

International Journal of Pharmaceutics

journal homepage: www.elsevier.com/locate/ijpharm

Review

Contact drying: A review of experimental and mechanistic modeling approaches

Ekneet Kaur Sahni [a], Bodhisattwa Chaudhuri [a,b,*]

[a] Department of Pharmaceutical Sciences, University of Connecticut, Storrs, CT 06269, United States
[b] Institute of Material Sciences, University of Connecticut, Storrs, CT 06269, United States

ARTICLE INFO

Article history:
Received 6 February 2012
Received in revised form 2 June 2012
Accepted 2 June 2012
Available online 9 June 2012

Keywords:
Contact drying
PAT approaches
Mechanistic modeling

ABSTRACT

Drying is one of the most complex unit operations with simultaneous heat and mass transfer. The contact drying process is also not well understood as several physical phenomena occur concurrently. This paper reviews current experimental and modeling approaches employed towards a better understanding of the contact drying operation. Additionally, an overview of some fundamental aspects relating to contact drying is provided. A brief discussion of some model extensions such as incorporation of noncontact forces, interstitial fluids and attrition rate is also presented.

Contents

1. Introduction

Drying is a complicated process with simultaneous heat and mass transfer accompanied by physicochemical transformations. Drying occurs as a result of vaporization of liquid by supplying heat to wet feedstock (Mujumdar, 2007). Although the importance of drying and its control has been recognized for many years, it is still more of an art than a science due to the intricacies involved in the process. To preserve the quality of the product, a balance must be achieved between the time of drying and product quality.

Based on the mechanisms of heat transfer, drying is categorized into direct (convection), indirect or contact (conduction), radiant (radiation) and dielectric or microwave (radio frequency) drying. Direct or the adiabatic units use the sensible heat of the fluid that contacts the solid to provide the heat of vaporization of the liquid. In contrast, contact dryer is an indirect method of removal of a liquid phase from the solid by application of heat such that the heat transfer medium is separated from the product to be dried by a metal

Abbreviations: APIs, active pharmaceutical ingredients; DEM, discrete element method; DPM, distributed parameter models; GC, gas chromatography; HPLC, high performance liquid chromatography; KF, Karl Fischer; LOD, loss on drying; LPM, lumped dynamic models; NIR, near-infrared; NIRS, near-infrared spectroscopy; NMR, nuclear magnetic resonance; ODE, ordinary differential equations; PAT, process analytical technology; PDE, partial differential equations; PM, penetration model; TGA, thermo-gravimetric analysis; TPD, thermal particle dynamics.

* Corresponding author. Tel.: +1 860 486 4861; fax: +1 860 486 2076.
E-mail address: bodhi.chaudhuri@uconn.edu (B. Chaudhuri).

0378-5173/$ – see front matter © 2012 Elsevier B.V. All rights reserved.
http://dx.doi.org/10.1016/j.ijpharm.2012.06.010

Nomenclature

$\dot{m}$	drying rate, kg m^{-2} s^{-1}
p	pressure in dryer, bar
p_b	bulk pressure, bar
p_s	saturation pressure at drying front, bar
q_o	heat flux into bed, W m^{-2}
q_{zT}	heat flux into drying front, W m^{-2}
T_b	bulk temperature, K
T_o	interfacial temperature, K
T_s	saturation temperature, K
T_w	hot surface temperature, K
α_p	particle heat transfer coefficient, W m^{-2} K^{-1}
α_{sb}	bulk heat transfer coefficient, W m^{-2} K^{-1}
α_{ws}	contact heat transfer coefficient, W m^{-2} K^{-1}
β_b	bulk permeation coefficient, m s^{-1}
β_p	particle permeation coefficient, m s^{-1}

wall (Root, 1983). Heat transfer to the product is predominantly by conduction through the metal wall and/or the impeller. Therefore, these units are also called as conductive and/or non-adiabatic dryers. Different types of heat transfer fluid may involve condensing (such as steam, hot gas, and diphenyl fluid) or liquid types (e.g. hot water and glycol solutions such as propylene glycol). Radiant dryers utilize radiation from a hot gas or a surface as the primary source of heat transfer, whereas in dielectric dryers, microwaves or high frequency electromagnetic fields are employed to transfer energy and achieve drying (Root, 1983; Malhotra and Okazaki, 1992).

Although more than 85% of the industrial dryers are of the convective type (Mujumdar, 2007), contact dryers offer higher thermal efficiency and have economic and environmental advantages over the convective dryers. Table 1 lists and compares the advantages of direct vs. indirect dryers (Root, 1983; McCormick, 1988; Uhl and Root, 1962; Malhotra, 1989). An important advantage of indirect dryers is lower energy consumption. Moreover, several energy resources can be utilized (condensing or liquid type), unlike the direct dryers that typically use light fuel-oil or natural gas. Tables 2 and 3 illustrate the selection criteria and solids exposure time respectively for various contact dryers. The main challenge associated with contact dryers is that they are difficult to design and engineer (Malhotra and Okazaki, 1992). An article by McCormick (1988) explains in detail the handling capacities of dryers (both direct and indirect) and how to choose the right unit for specific needs.

The authors do not intend to discuss the fundamentals of drying in the current review. The reader is referred to the textbooks, principles and practices in drying by Keey (1972) and the handbook of industrial drying by Mujumdar (2007) which provide a comprehensive description of the basic principles of drying processes with different types of dryers. This current review is limited, to the contact drying process, mainly concentrating on the approaches; both experimental and modeling, used in the literature to understand the physics behind the process and briefly discusses the parameters affecting the drying process. To this end, some of the fundamental aspects are reviewed briefly, including a short overview of the commonly used experimental and modeling approaches. Next, a review of relevant process analytical technology and recent modeling techniques are discussed at length, including some extensions of the modeling approaches, such as modification of the existing model to study drying in agitated, packed and intermittent stirred beds, as well as incorporation of noncontact forces and interstitial fluid effects. As the scope of the study is confined to the granular beds where contact drying is the primary mode of drying, direct dryers viz., spray, fluid bed, flash, tray and tunnel are excluded from the article. The review focuses primarily on simple indirect dryers, viz., paddle, disc type, filter dryer, and vibrated fluidized bed dryer. The information gathered from the literature is illustrated in tables to aid and equip the reader with a knowledge of practices that have been used in the past.

2. Background

Drying, being an integral part of pharmaceutical manufacturing is a bottleneck of the manufacturing process because of long drying times (Murru et al., 2011). Moreover, the product quality often depends on drying conditions and efficiency. In order to increase the driving force required for heat transfer, drying rates can be increased by increasing the jacket temperature and reducing the head-space pressure, in addition to mechanical agitation of the granular bed (Michaud et al., 2007; Michaud et al., 2008a,b). However, many pharmaceuticals are thermo-labile. Additionally, phenomena such as attrition and agglomeration can take place during extreme drying conditions, which may have a major impact on the functionality as well as the quality of the material being dried (Lekhal et al., 2003, 2004). Hence, in order to preserve the quality of the product, it is important to understand the parameters influencing the drying operation so one may achieve the most favorable conditions and avoid excessive drying. There are few reports in literature that deal with different types of contact dryers to evaluate the effect of process parameters (Malhotra and Mujumdar, 1987; Malczewski and Kaczmarek, 1989; Sztabert, 1989; Suzuki et al., 1985). Despite the perceived high industrial importance of vacuum contact drying, reliable correlations for the prediction of drying behavior in a dryer of a particular geometry are not available (Malhotra and Okazaki, 1992).

Contact dryers are generally preferred for heat sensitive materials such as foods, pharmaceuticals, and other biomaterials. Drying is also an essential part of the manufacturing process for active pharmaceutical ingredients (APIs). Contact drying is one of the least understood drying processes (Slangen, 2000) because several physical phenomena occur simultaneously (Whitaker, 1977, 1980). The drying kinetics depends on two different groups of parameters: operational conditions and material properties. In contact drying, the wet material is held as a layer in contact with heated surfaces, and the heat required for the evaporation of moisture is transported into the material by conduction (Mujumdar, 2007; Lachman et al., 1990). The residual solvent content of a material, usually expressed as percentage of the weight of the dry material, may be present as either free or unbound moisture. Unbound moisture which is in excess of the equilibrium moisture content is relatively easy to evaporate. Bound moisture is moisture that exerts a vapor pressure less than that of the free solvent at the same temperature (Malhotra, 1989). Such solvent may be physically or chemically adsorbed to the material and is more difficult to remove. Typically drying consists of three stages, i.e., the preheating, constant rate period and falling rate period (Lachman et al., 1990) as shown in Fig. 1 for moisture content vs. drying time and for drying rate vs. moisture content. In the preheating period, the unbound moisture in contact with the heated surface is evaporated. After this initial heating up period, the maximum drying rate is attained. This period is further followed by a constant rate period during which the drying rate remains constant and the unbound moisture is being evaporated; the decrease in the drying rate is caused by a reduction of heat transfer into the bed as the solids dry out. In the falling rate period, the drying rate continues to decrease until the bound moisture is removed. The temperature of the bed continuously increases to approach the temperature of the heat exchange surface. The first drying period is determined by temperature and velocity of the drying air; the second drying period depends mostly on the internal structure of

Table 1
Comparison of direct vs. indirect dryers.

Property	Direct/adiabatic dryer (convective type)	Indirect/nonadiabatic/contact dryer (conductive type)
Carrier gas	Uses sensible heat of gas that contacts the solid to provide the heat of vaporization of the liquid	Little or no carrier gas is required to remove the vapors released from the solids
Heat transfer	Heat transfer media is in direct contact with the surface of the material to be dried	Heat needed to vaporize the solvent is transferred through a wall
Risk of cross-contamination	Persists	Avoided, as the heat transfer medium does not contact the product
Solvent recovery	Difficult as there is large volume of gas to be cooled to recover the solvent	Easier because of limited amount of noncondesable gas encountered
Operation under vacuum	Not possible	Allow operation under vacuum, ideal for heat sensitive materials
Dusting	High	Minimized because of small volume of vapors involved
Explosion hazards	Higher rate	Easier to control as vapors can be easily condensed
Handling of toxic materials	Not suitable because of above mentioned reasons	Suited to toxic handling because of low gas flow
Energy efficiency	Low energy efficiency because high energy is lost through exhaust gas	Higher energy efficiency as the energy lost through the exhaust gas is greatly reduced
Evaporation and production rates	Higher Evaporation and Production rates in comparison to contact dryers	Drying rates are limited by heat transfer area; lower production rates (The maximum size of contact dryer is restricted as the surface: volume ratio of dryer decreases with increasing scale)
Cost	High	Higher initial cost Difficult to design, fabricate and maintain

Table 2
Selection criteria for the indirect dryers.

Dryer type	Plate	Drum	Tumbling	Vibrating	Conical	Thin film	Paddle	Mixer-kneader
Requirements								
Continuous	x	x	–	x	–	x	x	x
Discontinuous	–	–	x	–	x	–	x	x
Vacuum	x		+		x	x	x	x
Large surface area/volume	+	o	o	o	+	+	+	x
High specific capacity	+	x	o	x	+	x	+	x
Materials								
Friable	x	–	x	x	x	+	x	x
Fluid	–	x	–	–	–	x	o	x
Viscous/pasty	–	x	–	–	–	–	o	x
Crusty	–	x	–	–	–	o	+	x
Processing								
Mechanical	x	x	x	o	x	+	+	+
Thermal	+	o	o	+	+	x	o	o

–, not suitable; o, sometimes suitable; +, good; x, ideal (Source: Thurner, 1993).

the solid. Some moisture is still present at the end of the drying cycle. This residual moisture represents the lowest possible moisture content achievable under a given set of drying conditions and is called as the equilibrium moisture content.

The experimental techniques used to characterize drying are extremely diverse and in many cases are very specific due to the range of investigations and drying characteristics. Numerous off-line techniques have been used in the pharmaceutical and chemical industry to measure the residual solvent content. The existing methods for determining the end point of drying processes have involved either stopping at a predetermined time in order to collect the residual solvent content or continuing, at risk, to the next unit operation. The residual solvent content, collected during the drying process for various samples can be determined by loss on drying assay (LOD). LOD assay detects the loss of any volatile substance and is calculated by placing a known amount of sample in a tared container and drying it in an oven until a constant weight is attained. Thereafter, the samples are weighed again, and the loss in mass is the residual solvent content of the respective sample. Karl Fischer (KF) assay is used for the determination of water (Connors, 1988). It is based on the chemical reaction of iodine in the presence of water (Mujumdar, 2007; Keey, 1972). Both these conventional methods are time consuming. The time required for LOD can be as long as several hours. Water content may also be determined by head space analysis using gas chromatography (GC), where the sample is transferred in a sealed vial and heated up to a defined temperature. The head space is analyzed for water when equilibrium between the sample and the vapor phase is reached. Other off-line

Table 3
Solids exposure time of some indirect dryers.

Typical residence time of dryer	0–10 s	10–30 s	5–10 min	10–60 min	1–6 h
Thin-film contact	x	x	x		
Cone, batch				x	
Drum		x			
Steam-jacket rotary				x	
Tray, batch					x
Tray, continuous				x	

Source: Kimball (2001).

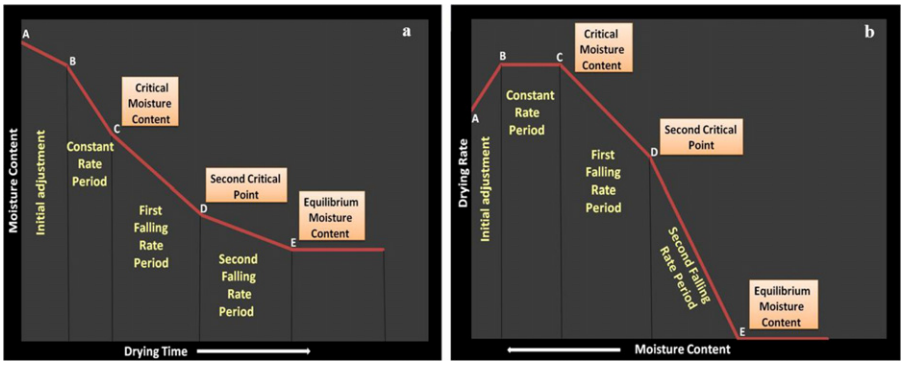

Fig. 1. Illustrates the periods of drying using (a) moisture content vs. drying time and (b) drying rate vs. moisture content (Lachman et al., 1990).

analyses, such as thermo-gravimetric analysis (TGA), high performance liquid chromatography (HPLC), nuclear magnetic resonance (NMR), or gravimetric analysis are also used to analyze the residual solvent content. The main disadvantage associated with the off-line measurements is that they require breaking the vacuum for sampling of wet cake. Replacing the above mentioned slow traditional methods (KF, TGA, etc.) with rapid, non-destructive methods would help improve the quality of the finished product. Published guidance for industry for process analytical technology (PAT), proposed by the FDA, (www.fda.gov, 2004) explains that the goal of PAT is to enhance the understanding and control the manufacturing processes and therefore facilitate "Quality by Design", or QbD. QbD is intended to design in quality rather than achieve quality by extensive testing of the products. Pharmaceutical companies are encouraged to incorporate PAT into development and manufacturing through the use of in-line and on-line monitoring tools (At-line measurements involve removing the sample, isolating from, and analyzing in close proximity to the process stream; on-line measurements refer to methods where the sample is diverted from the manufacturing process, and may be returned to the process stream, and in-line measurements denote methods where the sample is not removed from the process stream). Hence, implementation of the tools for on-line monitoring of drying processes minimizes the time the product spends in the dryer, thereby relieving the product of the stresses encountered from overdrying (Parris et al., 2005). Therefore, on-line monitoring tools reduce the cycle time and cost, allowing improved process control. These techniques provide valuable information regarding the process; however, each has its own limitations in terms of ease of operation, speed, and accuracy.

With the industry aspiring to improve manufacturing adeptness by adoption of PAT, it is important to consider sound approach to improve product quality; that is the use of process modeling. In the long term, use of process models provide critical process understanding as simulations bring much deeper insight into the impact of process variables on process economics and product quality and, henceforth, help to predict outcomes without running costly and labor-intensive experiments. Moreover, the benefits are also seen in reduced developmental resources and manufacturing costs, without any production delays. Different modeling techniques for contact drying (both in agitated and packed beds) have been employed over the past three decades. Two main genres of parameter models include distributed and lumped or concentrated. Distributed-parameter models (DPM) have at least one spatially independent variable and some Cartesian coordinates. DPM also have time as an additional independent variable. Hence, the state variables (temperature and moisture distributions) are functions of both time and space, and the model therefore has the form of partial differential equations (PDE's). Conversely, in lumped-parameter models (LPM) the state variables (temperature and moisture distributions) are not measured and instead spatially averaged measurements are used. Lumped dynamic models have only time as their independent variable leading to ordinary differential equations (ODE) (Michaud et al., 2008a,b). The most used and cited models are discussed in section 3.2 where the discussions include a short description of each of the modeling techniques.

3. Characterization of drying performance in contact dryers

3.1. Experimental techniques

An overview of the practices generally utilized in characterizing contact drying is presented in Table 4. During the last decade, both molecular vibrational spectroscopic techniques, viz. near infrared (NIR) and Raman spectroscopy have been increasingly used as process analyzers for real-time measurements of critical process and product attributes in pharmaceutical processing. These spectroscopic techniques allow rapid and nondestructive measurements without sample preparations. Both vibrational techniques can be complementary. NIR and Raman spectra also contain qualitative and quantitative information on the chemical composition as well as the physical properties (e.g., particle size and shape distribution) of the measured sample (Ciurczak et al., 1986; Rantanen and Yliruusi, 1998; Wang et al., 2002; Hu et al., 2006). This section reviews some of the studies concerning these spectroscopic techniques.

3.1.1. Near-Infrared spectroscopy (NIR)

For a number of years, NIR spectroscopy has been used for qualitative and quantitative measurements in the food and chemical industries. It is also a well-established tool within the pharmaceutical industry in applications involving inspection of incoming raw materials to the final testing of manufactured products. Being widely used for qualitative and quantitative measurements, both off-line and on-line, it is one of the PAT tools used to gain a more complete understanding of pharmaceutical processes leading to a higher throughput while reducing the risk of out-of-specifications batches. In situ monitoring brings additional benefits of eliminating the requirement for sampling, thereby reducing the analytical efforts and hence the exposure of operators to products (Workman and Weyer, 2008).

NIR spectroscopy covers the electromagnetic spectrum between 780 and 2526 nm (12,820–3959 cm^{-1}). The peaks observed in NIR spectra arise mostly from the absorption bands due to overtones and combinations of the fundamental modes of –CH, –NH, –OH (and –SH) functional groups (Fig. 2, Siesler, 2002). NIR spectroscopy allows rapid, non-destructive and non-invasive measurements. In NIR spectroscopy, the samples are irradiated with NIR light some of which is absorbed by the molecules, bringing them to a higher vibrational state as shown in Fig. 2. Only the vibrations resulting in

Table 4
Experimental techniques to characterize drying performance.

Experimental techniques	Information	Advantage	Disadvantage
Off-line techniques Such as: LOD, Karl Fischer (Connors, 1988), TGA	Residual solvent content	• Simple and easy to operate	• Time consuming • Requires breaking vacuum at individual time points and sampling of the wet cake. • Cannot provide real-time water levels during the drying of a drug substance
On-line Near-Infrared (NIR) (Bakeev, 2004; Shering, 2005; Parris et al., 2005; Kogermann et al., 2007; Bellamy et al., 2008a, 2008b; Burgbacher and Wiss, 2008)	The samples are irradiated with NIR light some of which is absorbed by the molecules, bringing them to a higher vibrational state.	• Rapid and non-destructive	• Baseline shifts interfere with calibration development complicating the analysis
		• Contain qualitative and quantitative information • Offers the opportunity to monitor changes in the particle bed during the evaporation of solvent	• Influence of physical properties on spectra • Main problems associated with collecting representative spectra
		• Eliminates the need for multiple, in-process sampling during drying, thus speeding up the process	• Affected by water and particle size
		• Online monitoring improves the cycle time and reduces the analytical work as well as cost	• Poor fingerprint
Raman spectroscopy (Walker et al., 2009; Beer et al., 2011; Hamilton et al., 2011)	The amount of "polarizability" of the bond determines the intensity and frequency of the Raman shift. Raman spectrum displays the frequency difference between the incident radiation and the scattered radiation, expressed as wavenumbers.	• No sample preparation	• A challenge to visual interpretation is the irregular nature and varying magnitude of a small baseline
		• Rapid and non-destructive	• Often restricted by its need for chemometric models
		• Contain qualitative and quantitative information on the chemical composition as well as the physical properties • Monitor changes in the particle bed during the evaporation of solvent • Narrow spectral features • Simpler interpretability • Water does not interfere significantly with the vibrational bands of the drugs i.e. water is Raman inactive • Higher resolution compared to other at-line techniques	

changes in dipole moment (product of positive or negative charges and distance) of a molecule can absorb NIR radiation.

NIR spectroscopy measurements are performed either in diffuse reflectance or transmission mode, or in combination of the two-transflection mode. Diffuse reflectance is more widely used for solid-state analysis (Lodder and Hieftje, 1988), but problems related with quantitative assessment of bulk solid dosage forms, such as inhomogeneity of the sample, have shifted the interest to the use of the transmission mode. There are also difficulties associated with transmission measurements, such as a relatively small wavelength region available for analysis related to the absorption coefficient of the material (Gottfries et al., 1996). However,

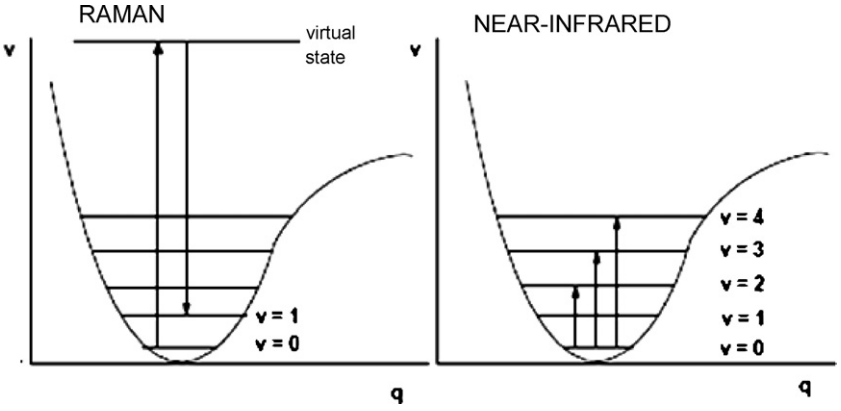

Fig. 2. Vibrational energy level diagram for Raman and NIR spectroscopy, (Siesler, 2002); v vibrational quantum number, q vibrational coordinate; $\nu = 0$ (ground state), and $\nu = 1, \nu = 2, \ldots, n$ (excited states).

transmission mode NIR spectroscopy is suitable for intact tablet assessment (Lodder and Hieftje, 1988; Abrahamsson et al., 2005). The absorption bands in NIR spectra are broad, overlapping and weak. Therefore, NIR spectroscopy requires use in combination with multivariate analysis methods, which extract the relevant information from the spectra (Stephenson et al., 2001). NIR spectroscopy measurements are more suitable for the analysis of major components because of lower sensitivity. Further details on NIR can be found in the literature (Siesler, 2002; Workman and Weyer, 2008; Beer et al., 2011).

NIR spectroscopy displays information from the intramolecular vibration changes in the crystal thereby revealing information about the physical (particle size, density, morphology, temperature) and chemical properties (vibrations linked with hydrogen bonding) of the sample (Reich, 2005). Moreover, NIR spectroscopy is extremely sensitive to water. Water gives the strongest absorption bands approximately at 1940 (5150 cm^{-1}) and 1450 nm (6900 cm^{-1}). NIR spectroscopy further enables differentiation between free water and structural water. The shift to a higher wavelength occurs with hydrogen bonded water (Räsänen et al., 2001). Therefore, utilizing this sensitivity to water, hydrates are usually easily distinguished from anhydrous forms.

Bakeev (2004) discusses the at-line and on-line applications as well as implementation strategies of NIR. Moisture measurements are widely quantified by NIR. At-line measurements are generally made for lyophilized products and for tablets whereas on-line applications in the pharmaceutical industry are often made for actives. Although most of the earlier manuscripts describe the implementation of NIR in fluidized bed granulators (Frake et al., 1997; Rantanen et al., 1998; Green et al., 2005; Findlay et al., 2005), NIR has also been used to monitor drying progress in order to optimize the process and detect the end of drying. Additionally, it has been used to measure the total water, surface as well as the bound water in drug substances during the drying processes (Zhou et al., 2003).

Another article describes the evolution of a sampler for NIR to monitor drying in pressurized filter dryers (Shering, 2005). Astra Zeneca developed the concept of a retractable NIR probe in collaboration with Clairet Scientific and ABB Bomem. In order to get the optics inside the cake, the retractor mechanism allows the probe to be withdrawn when the agitator is in operation. Although the probe failed to penetrate some crusted areas, no problems were encountered once the cake was agitated. In order to establish the best technique to collect the spectra, product samples were collected following different sampling regimes like with/without agitation, various agitation times, with repeated insertion of probes, etc. Although the results demonstrated that representative spectra could be collected from a single insertion into the homogenized cake, but the objective of obtaining good spectra from a representative sample still remains elusive (Dr. Philip Shering, personal communication).

Parris and coworkers (2005) explained the operation and performance of a miniaturized NIR analyzer in monitoring a drying process for APIs. Their work involved drying an API wetted with two solvents, dichloromethane and n-heptane. Solvents were detected individually with this NIR method. The spectrometer was employed, based on a superluminescent diode source, with a MEMS Fabry-Perot tunable filter and an In-GaAs detector. Each scan of the spectrometer was wavelength and absorbance referenced in order to provide accurate and reproducible spectral measurements. Monitoring the decrease of solvents in the gas stream using spectral features was complicated due to baseline shifts. The spectral data collected were evaluated using multivariate calibration methods (partial least squares regression). Hence, implementing an on-line NIR tool facilitates the monitoring of a critical process attribute, such as the completion of drying. Therefore, most of the solvents used to produce APIs can be detected using NIR spectra and analyzed using chemometric data analysis. Their studies showed that the solvent concentrations determined using NIR were in good agreement with the reference analyses.

Burgbacher and Wiss (2008) demonstrated the effectiveness of NIR to control drying processes on an industrial scale. They described a method to monitor the drying curve using different kinds of dryers (filter dryer, paddle dryer and spherical dryer) and various solvents (water and organic solvents). A diffuse reflectance probe was placed flush with the internal wall of the dryer and spectra were recorded once every 10 min. The spectral data were evaluated employing multivariate calibration methods to determine the solvent concentrations during drying, resulting in reduction in cycle time. The solvent concentrations determined using NIR were in good agreement with the reference analyses with KF and GC. Although NIRS data are known to contain particle size information (Kogermann et al., 2007; Bellamy et al., 2008a,b), there was no discussion of the effects of drying on particle size in their study.

The main drawback of the NIR technique is the complexity of the spectra due to their origin (overtones and combination bands of vibrational energy levels) which can result in a broad range of overlapping absorption bands making it difficult to obtain relevant information at only one wavelength (Luypaert et al., 2007).

3.1.2. Raman spectroscopy

Raman spectroscopy typically involves the region between 4000 and 200 cm^{-1}. The Raman measurement essentially involves irradiating the sample with monochromatic laser light and interaction with the electron cloud of the bonds of that molecule. The amount of deformation of the electron cloud is referred as the "polarizability" of the molecule. The energy of this light is higher than the energy needed to bring molecules to a higher vibrational state (Beer et al., 2011). Most of the incident radiation is scattered by the sample molecules at the same frequency. This identical scattered light is called Rayleigh radiation. Some light is scattered inelastically by the sample molecules reflecting that energy exchange occurred between the incident light and the sample. This inelastic scattering is called the Raman effect. This inelastic scattered radiation can have a lower energy (lower frequency) than the incident radiation referred to as Stokes radiation or a higher energy (higher frequency) than the incident radiation, termed anti-Stokes radiation as shown in Fig. 2. The amount of "polarizability" of the bond determines the intensity and frequency of the Raman shift. Hence, Raman spectrum displays the frequency difference between the incident radiation and the scattered radiation, expressed as wavenumbers, versus the intensity of the scattered radiation. The molecule under investigation must be symmetric to observe the Raman shift (Chao et al., 1974). Theoretical background of the Raman spectroscopy is quite well established and described in the literature (Long, 1977; Gardiner et al., 1989). Every compound gives a unique spectrum arising from excitation of the vibrational modes of the molecule and for mixed samples the spectra are a superposition of the signals from each of the constituents.

Typically, the Fourier transform Raman (FT-Raman) or dispersive Raman techniques are applied (McCreery, 2000) to collect the Raman spectra. The techniques differ basically in the laser source and in the way Raman scattering is detected and analyzed. Raman spectroscopy is useful in determining the molecular structure, characterizing different solid-state forms, determining the hydration states, and in studies of solid-state phase transitions. It can be employed for both qualitative and quantitative analysis of pharmaceuticals (Pelletier, 2003).

Studies in the literature (Kogermann, 2008) revealed that vibrational spectroscopy together with multivariate modeling can be used to monitor and investigate dehydration behavior in situ

Table 5
Computational techniques used to model contact drying operation.

Computational techniques	Information	Advantage	Disadvantage
Penetration model (Schlünder, 1980; Mollekopf and Schlünder, 1982; Schlünder and Mollekopf, 1984; Tsotsas and Schlünder, 1986, 1987; Forbert and Heimann, 1989; Heimann and Schlünder, 1988; Kohout et al., 2006, 2007; Michaud et al., 2008a,b)	It is continuum approach, where the steady mixing process is replaced by a sequence of unsteady mixing steps. Hence during the static period a distinct 'drying front' is penetrating from the hot surface to the bulk, such that all the particle are dry between the moving front and hot surface and beyond the front, all are wet.	• Simple to operate	• Requires adequate experimental data for its use
		• Easy extension to contact drying applications	• The penetration model fails to reveal the behavior of individual particles and does not consider inter-particle interactions • Cannot describe deterministic patterns of particle motion • Scale-up is difficult
Pore Network technique (Nowicki et al., 1992; Laurindo and Prat, 1998; Plourde and Prat, 2003; Segura and Toledo, 2005; Metzger and Tsotsas, 2005; Irawan et al., 2005; Metzger et al., 2005)	Accounts for different phenomena occurring at the pore scale.	• Flexible model	• Qualitative in nature
		• Describe the drying of porous media at the pore level	• Main challenges associated is that it does not account for all the transport effects • A lot of drying information should be incorporated into the effective parameters of networks
Population Balance (Burgschweiger, 2000; Burgschweiger and Tsotsas, 2002)	These define how populations of separate entities develop in specific properties over time. It gives the behavior of a population of particles from the analysis of behavior of single particle in local conditions.	• Population balances model the evolution of properties that may differ from particle to particle	• A lot of experimental data is required
		• Simple approach	• One-dimensional approach
Discrete element modeling (DEM) (Cundall and Strack, 1979; Vargas and McCarthy, 2000, 2001; McCarthy and Ottino, 1998; Kwapinska et al., 2005)	Predict trajectories of all particles using Newton's equations of motions and Euler's law	• Provide dynamic information (transient forces) which are difficult to calculate experimentally	• Time intensive process
		• Predictions outside the range of immediate use are likely to be accurate • Effect of non-spherical particles, effects of geometry (design of baffles), vessel internals, and the formation of liquid bridges all can be modeled	• Vast inherent computational intensity • Limited number of particles

and in-line during the unit operation, fluidized bed drying. NIR and Raman were used to monitor the solid-state transformations, and multivariate data analysis was performed to interpret the spectral information. The goal was also to predict and quantify the multiple solid-state transformations in-line during drying. Raman spectroscopy detects mostly the intramolecular vibrations revealing information about the crystal structure changes. Raman spectroscopy was found to have higher spectral resolution, which allowed quantifying two piroxicam (PRX) forms and all four carbamazepine (CBZ) solid state forms during isothermal dehydration. NIR spectroscopy, on the other hand, was more sensitive to water content and the hydrogen bonding environment of water molecules. NIR spectroscopy revealed complementary information about the dehydration from PRX monohydrate to PRX anhydrate form I, showing good agreement with Raman spectroscopy and TGA results. However, NIR spectroscopy was incapable of differentiating between the anhydrous solid-state forms of CBZ during dehydration. Hence, NIR spectroscopy models could quantify the solid-state forms in the binary system, but were unable to quantify all the forms in the quaternary system.

Raman spectroscopy offers advantages over NIRS by providing narrower spectral features and simpler interpretation. More recently, in situ measurements by Raman spectrometry during monitoring removal of methanol from needle-shaped particles of D-alpha cellobiose octaacetate (COA) in a vacuum agitated filter dryer were described in detail by Hamilton et al. (2011); these studies illustrated the use of combined drying curves to study the effects of drying parameters (method of agitation, % solvent loss on drying and jacket temperature). The drying curves based on Raman data provided an indication of the end of drying and revealed three stages in the drying process; these data were used to monitor the progress of solvent removal in real time and facilitated rapid optimization of process parameters. The study demonstrated that it was possible to extrapolate experimentally derived information to predict both the extent of attrition and the drying time for a given combination of drying temperature, percent loss (of solvent) on drying, and mode of agitation. Off-line Raman analysis and particle size analysis were used as reference measurements. A correlation between particle size and off-line Raman measurements of COA was established. However, it was not possible to derive equivalent

information from the in situ Raman spectra owing to the greater effects of particle motion or bulk density variations of the particles in the dryer. Although continuous agitation gave shorter drying times, intermittent agitation reduced the degree of particle attrition throughout the process. Particle size effects on the Raman signal for COA studied with off-line analysis were associated with the differences in the packing of the large and small particles.

3.2. Modeling approaches for contact drying processes

There are drying models of different complexity, each with a particular set of equations connecting all the process parameters and material properties describing the behavior of the system. As mentioned before, drying models are classified as distributed and lumped parameter models. Distributed-parameter models can further be categorized as either continuum or discrete. In continuum models, the heat and mass transfer phenomena are described by macroscopic laws with constant or variable effective transport properties (Kohout et al., 2006). In contrast, the heterogeneous microstructure of the porous medium is explicitly represented in discrete models, either by a pore network model (Wei et al., 1987; Metzger et al., 2005) or by the reconstructed porous medium approach (Kosek et al., 2005). Table 5 presents an overview of the modeling approaches including a short description as well as advantages and limitations of each approach.

3.2.1. Penetration model (PM) and Vaporization front model

3.2.1.1. Drying studies in mechanically agitated beds. Since the 1980s, Ernst Ulrich Schlünder and coworkers have contributed significantly to the understanding of contact drying operations in mechanically stirred granular beds. They carried out systematic investigations for hygroscopic and nonhygroscopic beds of fine and coarse free flowing particles (Schlünder, 1980; Mollekopf and Schlünder, 1982; Schlünder and Mollekopf, 1984; Forbert and Heimann, 1989; Heimann and Schlünder, 1988). These investigations were further extended by Tsotsas and Schlünder (1986, 1987) and by Farges et al. (1995) for poly-disperse and hygroscopic materials, respectively. Studies concentrating on vacuum contact drying of free flowing, mechanically agitated granular beds showed that the drying rate was affected by both heat supply and vapor removal. Drying rate was shown to be a function of vapor pressure, heated surface temperature, stirrer speed and moisture content (Schlünder, 1980; Mollekopf and Schlünder, 1982; Schlünder and Mollekopf, 1984). The heat supplied must overcome three heat transfer resistances: the contact resistance at the hot surface, the bulk penetration resistance and the penetration resistance of the particle. Vapor removal must overcome two mass transfer resistances: the permeation resistance of the particles and the permeation resistance of the bulk. For a packed bed, all the above mentioned resistances lie in series as shown in Fig. 3. However, if the particulate material is mechanically agitated, a random distribution of dry, partly wet and wet material is expected to form a random distribution of transport resistances partly in series and partly in parallel. The heat and mass transfer resistances are illustrated in Fig. 3.

Heat transfer resistances:

Contact:

$$\frac{1}{\alpha_{ws}} = \frac{T_w - T_o}{q_o} \tag{1}$$

Bulk penetration:

$$\frac{1}{\alpha_{sb}} = \frac{T_o - T_b}{q_o} \tag{2}$$

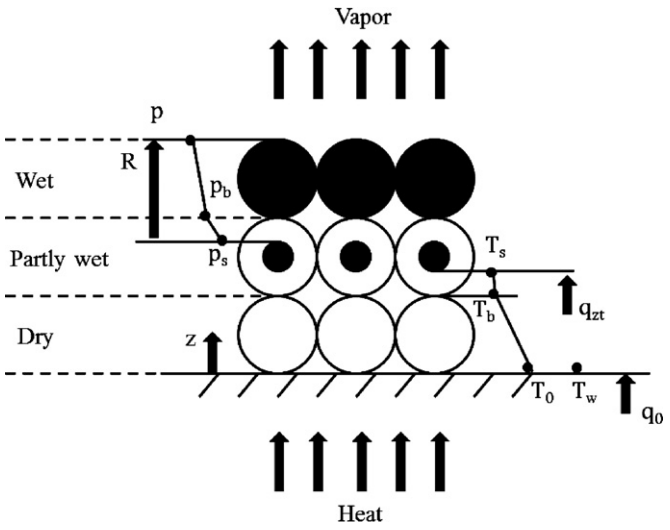

Fig. 3. Shows the heat and mass transfer resistances in contact drying (Schlünder and Mollekopf, 1984)

Particle penetration:

$$\frac{1}{\alpha_p} = \frac{T_b - T_s}{q_{zT}} \tag{3}$$

Mass transfer resistances:

Particle permeation:

$$\frac{1}{\beta_p} = \frac{p_s - p_b}{\dot{m}} \tag{4}$$

Bulk permeation:

$$\frac{1}{\beta_b} = \frac{p_b - p}{\dot{m}} \tag{5}$$

The granular bed is considered to be randomly mixed with mixing being achieved by the following possibilities discussed in detail by Schlünder and Mollekopf (1984):

(a) Perfect macromixing and perfect micromixing
(b) Perfect macromixing, still imperfect micromixing

The heat transfer from walls in mechanically agitated beds is usually described by a penetration model as illustrated in Fig. 4. In this approach, the bed of particles is viewed as a continuum with effective properties. The notion of the "penetration theory" is that of discretization of the continuous mixing process to a series of static periods with assumed instantaneous and perfect mixing in between. The duration of every fictitious static period is equal to t_R, after which perfect mixing is achieved instantaneously. During the static period a distinct 'drying front' penetrates from the heated surface into the bulk. Between this moving front and the hot surface, all the particles are dry, but beyond the front all the particles are wet. After perfect mixing is attained, the drying front starts to penetrate again from the surface and this cycle is repeated over and over again. However, for each repeat time, some particles behind the front have been dried already during the previous period. Some of the particles beyond the front have also been dried, thereby achieving a random mixture of dry and wet particles within the bed.

The length of the fictitious contact period, t_R is presumed to be a function of the time scale of the mixing device and hence

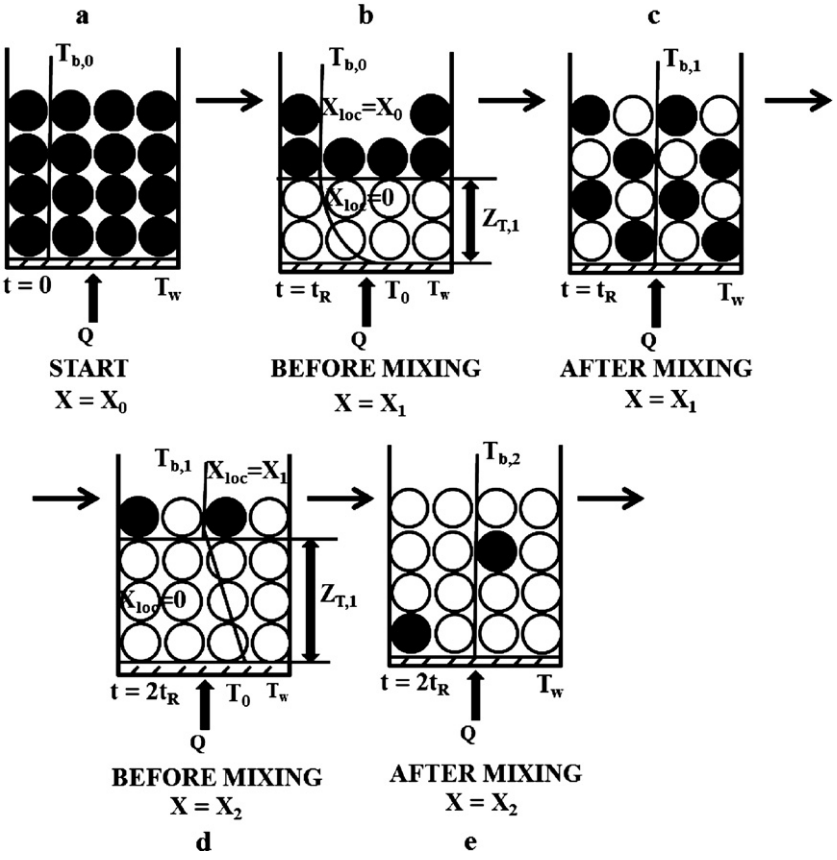

Fig. 4. Illustrates the contact drying model (Schlünder and Mollekopf, 1984)

characterizes the efficiency of mixing of particles. This duration is correlated with the rotational frequency, n of the mixing device:

$$t_R = t_{mix} N_{mix} \tag{6}$$

$$t_{mix} = \frac{1}{n} \tag{7}$$

Mixing number, N_{mix} expresses the number of revolutions necessary in order to achieve perfect mixing. The mixing number serves as a mechanical property of the mixing device connected with the mechanical properties of the product and is a function of the time scale of the stirrer.

$$N_{mix} = CFr^x \tag{8}$$

$$Fr = \frac{(2\pi n)^2 D}{2g} \tag{9}$$

where D is the diameter of the disc or drum, Fr is the Froude's number and g is the gravitational constant. Values of C and x are evaluated from the experimental data.

Schlünder and Mollekopf (1984) estimated the performance of following contact dryers: two disc dryers with stirrers, a rotary drum dryer and a paddle dryer. The theory was based on the assumption that the drying rate is dominated by two heat transfer resistances i.e. contact and bulk resistance. With the use of this model, good agreement was obtained between theory and experiments for five different contact dryers (disc, drum and paddle) of various sizes (1.1 to 160 L), operated at various pressures (1–200 mbar), different temperatures (10–200 °C), various mixing times ($0.2\,rev\,min^{-1} \le n \le 130\,rev\,min^{-1}$) and filled with different monosized free flowing fine as well as coarse material (diameters of 170 μm to 6.6 mm). Depending on the dryer type and the Froude number, the mixing number was found to lie between 2 and 25. The penetration model introduced by Mollekopf and Schlünder (1982) was extended to describe the influence of diameter disparity on the drying rate curve during vacuum contact drying of multigranular packing.

Experimental investigations have been carried out in a disc dryer by Tsotsas and Schlünder (1986) using free flowing bi- and poly-dispersed packings of porous granular material. As a result of variation in size or density, de-mixing of the components of the mixture occurs. The studies showed that as the contact heat transfer coefficient increases with decrease in particle size, drying rate for fine material was seen to be much higher than that for the coarse material. Over the past three decades, many authors have investigated heat transfer from the heated walls to the granular beds. Within these studies, a number of cases have been investigated. Tsotsas and Schlünder (1987) extended the penetration model developed by Schlünder and Mollekopf (1984) to account for the influence of bound moisture on the drying rate in a disc dryer. The applicability of the extended model was subject to the following limitations: prediction of the mixing number, N_{mix} and intraparticle resistances to heat and mass transfer was not considered (Heimann and Schlünder, 1988). To evaluate the outcomes of a variation of drying conditions (wall temperature, pressure), mixing intensity (stirrer speed), granular bed properties (bed height, particle diameter), and the physical properties of the moisture, the following characteristics quantities were used: the dimensionless contact time, the characteristic number of liquid-phase mass transfer, and the dimensionless residence time of the vapor in the bed. Although empirical correlations are available in the literature to allow the mixing number to be related to the rotational frequency and apparatus diameter, this single parameter is not sufficient to completely describe the complex motion of particles where there are approximately six different regimes of particle motion

(depending on particle diameter, drum diameter, rotational frequency and loading).

Recently, Arlabosse and Chitu (2007) used the penetration model to simulate the drying kinetics of sewage sludge. In their study, vapor was used as sweeping gas during the contact drying experiment. Thus, mass transfer resistance in the gas phase was not taken into account. The authors considered the contact drying modeling of sewage sludge in sticky, lumpy and particulate phases in the presence of air. Their research suggests that the drying kinetics of sewage sludge can be adequately described by the model. In order to have a better understanding of the sewage sludge drying mechanism, a penetration model developed by Tsotsas and Schlünder (1986) was used to simulate the drying kinetics of the three distinct phases in the Nara-type paddle dryer: pasty, lumpy and granular phases. The influence of the drying parameters on the drying kinetics was investigated. Both the drying temperature and stirrer speed had a great influence on the drying kinetics in the examined range, whereas the air flow rate had little influence on the drying kinetics in the air flow rate range of 0.5–1.3 $m^3 h^{-1}$. The results indicate that the penetration theory satisfactorily describes the sludge drying kinetics of all phases. Further, Deng et al. (2009) studied the contact drying of sewage sludge in a Nara-type paddle dryer. The focus of their work was to validate the model for several real pharmaceutical compounds under a range of operating conditions (pressure, temperature) and for different solvents. In addition to that, they demonstrated its use in an integrated methodology for process scale-up that involves parameter identification at the laboratory scale and the prediction of drying times at the pilot or manufacturing scale. The model was indicated to be easily extensible to vacuum drying with intermittent agitation of the filter cake. In spite of similar trends obtained using the penetration model, they were unable to make accurate predictions because of the fitting of their central parameter, the mixing number, to the results of thermal experiments.

3.2.1.2. Drying studies in packed beds. Mechanical agitation can result in particle breakage and complicate the transport process during drying. Hence, mechanical agitation is sometimes avoided, and the drying occurs from a static particle bed. Static beds have been studied by Tsotsas (1985), Moyne (1987), Baillon (1996), and lately by Kohout et al. (2004, 2005). Vacuum contact drying of hygroscopic packed beds was conducted by Tsotsas (1985) with porous particles. The author did not observe any constant rate period as the falling rate period started as soon as drying began, presumably because the liquid transfer from the bulk to the heating wall was prevented because moisture was bound to the particles. Tsotsas (1985) developed a classical quasi-stationary "vaporization front" model to simulate the experiment. Furthermore, a detailed experimental study on packed bed vacuum contact drying was conducted by Moyne (1987) with pure water and 200 μm non-porous glass beads. Unlike the above mentioned study, four distinct periods of drying were observed: a short initial period during which both the bed temperature and drying rate increased; a classical constant rate period during which the bed at the heated wall remained saturated with solvent; a first falling rate period, starting from a critical moisture practically independent of operating conditions, and a second falling rate period during which the slope of the drying rate curve decreased to a greater extent as drying progressed. Further, the temperature profile during vacuum contact drying of a pharmaceutical granular packed bed was investigated by Baillon (1996). According to these studies, the temperature profiles inside the bed corresponded to two zones during the falling rate period: a dried zone near the heated wall (where the temperature gradient was high) and a wet zone (where the temperature gradient was much lower).

More recently, Kohout et al. (2005) experimentally investigated the effect of key process parameters (pressure, temperature, vessel dimensions, bed depth, and particle size) on the kinetics of vacuum contact drying a wet bed of non-porous particles. Kohout et al. (2006, 2007) developed a model to simulate the drying rates of non-porous glass beads packed in a cylindrical vessel. In their studies, empirical correlations relating the bed temperature to surface heat transfer coefficients for a range of operating variables have been proposed. However, such correlations are of restricted utility because they cannot be easily generalized to different equipment geometries, and it is risky to extrapolate their use outside the experimental range of the variables studied. Moreover, most of these models do not capture particle-surface and inter-particle interactions or the detailed microstructure of the granular bed. The drying rate in the constant rate period was found to be independent of the nature of the driving force, the jacket temperature or the headspace pressure. Heat transfer rate in the constant rate period was found to be a linear function of bed depth in two different diameter vessels. The overall heat transfer coefficient, however, is a nonlinear function of the bed depth and depends on the diameter of the vessel as well. Finally, particle size was found to have a very strong effect both on the drying rate and on the existence of the constant rate period. For the smallest particle size investigated, drying rate was found to be a function of moisture content even in the constant rate period. The drying rate decreased with increasing bed depth, but the absolute heat transfer rate in the constant rate period was an increasing function of bed depth as the number of contacts were more for smaller particles. Kohout et al. (2006, 2007) developed a general dynamic and a specific steady state model to simulate the drying rates of non-porous glass beads. Validity of the steady state model was applicable during the constant rate phase to the case where the liquid mass transfer to the heating wall by capillary flow was faster than the vapor mass transfer. During the constant rate phase, the vaporization phenomena occurred effectively in a thin zone near the heated wall. The drying rates were governed both by contact heat transfer at the heated wall and by solvent vapor mass transfer through the bulk of the granular bed. The average moisture content decreased from its original value to the percolation threshold value when redistribution of the liquid by capillary flow stopped and the falling rate period started. Further, the falling rate period was characterized by a sharp vaporization front moving from the heated wall through the bulk of the bed which was divided into two zones: a dry zone between the heated wall and the drying front; and a wet zone between the drying front as well as the free surface of the bed. The solvent content in the wet zone was assumed to be uniform with a value equal to the percolation threshold as in a classical vaporization front drying model.

Nastaj (1994) used a similar model to simulate the falling rate period during vacuum contact drying in packed beds. The typical "vaporization front model" was not representative of vacuum contact drying of lactose monohydrate and potassium chloride in packed beds during the falling rate period. Hence, a good agreement between simulations and experiments was obtained only when the bed depth was small (2 mm).

Malczewski and Kaczmarek (1989) investigated the vacuum contact drying of white and red clover seeds in vertical and horizontal type dryers at a wall temperature of less than 50 °C. They showed the superiority of the contact drying process in terms of reduced energy consumption (less than 50%) and increased product quality in comparison with purely convective process. A similar approach was also followed by Sztabert (1989) while drying the pharmaceutical products in a paddle-type dryer. Experiments on vacuum contact drying of a wet mass of non-porous particles have been reported by Skansi et al. (1997). The effect of pressure and temperature (three values of each parameter) on the drying rate of ketoprofen was investigated. However, the pressure and

temperature were treated as unrelated parameters and a purely empirical model was proposed. Studies performed in packed beds indicate that although increased contact time increases the drying rate, the product quality usually suffered from increased occurrence of hot-spots resulting from overheating of a particular part of the bed.

3.2.1.3. Drying studies with intermittent stirring. Physical phenomena such as attrition and agglomeration are induced in agitated drying by the difference in the moisture content during different drying stages. One of the major concerns and challenges in pharmaceuticals is the change in crystal size and shape from what is desired during the drying process. Size reduction occurs as a result of particles colliding with one another or with the walls and/or the agitator (Bemrose and Bridgwater, 1987; Keey, 1992; Neil and Bridgwater, 1994; Mazzarotta et al., 1996). Hence, attrition can seriously impact the subsequent blending and the tableting processes due to the poor flowability of fines generated throughout the process. Likewise, agglomerates are usually undesirable due to their low dissolution rate. Lekhal et al. (2003) studied the impact of drying conditions (temperature, agitation speed and vacuum) on drying characteristics (drying rate and time) and final crystal properties (size and shape distribution). They found that attrition dominated particle size changes when the drying rate was low and/or the shear rate was high, while agglomeration dominated when the drying rate was high. The influence of intermittent stirring on the drying rate was investigated by Michaud et al. (2007). Vacuum contact drying of lactose monohydrate and potassium chloride beds were experimentally investigated and numerically simulated. Drying rates and temperature profiles for different operating conditions (pressure, heating fluid temperature, duration of stirring "on" and stirring "off" periods) were determined in a laboratory vacuum contact dryer. The duration of periods with stirring and without stirring were optimized to obtain high mean drying rates with a low total stirring time in order to reduce the attrition and agglomeration phenomena (Michaud et al., 2008b).

Michaud et al. (2008a) investigated the duration of stirring periods below which the drying rate was too low. The classical "vaporization front" model was improved by incorporating the following modifications: the introduction of a jacketed vessel heat transfer coefficient and an accumulation term for the heating wall; the application of alternate static bed and stirred bed conditions; and the modeling of all the three drying phases, namely the constant rate, the transition, and the falling rate phase. The model development is comprehensively discussed by Michaud et al. (2007, 2008a). For the constant rate phase, the steady state model formerly proposed by Kohout et al. (2006, 2007) was selected. The drying rate was calculated by concurrently solving three steady state balance equations: Newton's law applied to heat transfer between the heating fluid and the wall, Darcy's law utilized for vapor transfer between the wall and the bulk of the bed and energy balance at the wall. The average solvent content decreased from the initial value to a first critical solvent content, at which the transition phase started. During the transition phase, the amount of liquid at the heated wall decreased but solvent vaporization occurred in a thin zone located near the heated wall. For the falling rate phase, drying periods without stirring were modeled based on the phase change front approach (Grigull and Sandner, 1984; Carslaw and Jaeger, 1959) for a one dimension semi-infinite medium. For periods with stirring during the falling rate, the model used was based on the "penetration theory" as described in detail by Schlünder and Mollekopf (1984). The basic assumptions of the phase change front approach were: the drying rate was entirely controlled by three thermal resistances starting from fluid to wall, wall to the first layer of particles, first particles to the bulk, and that a vaporization front moved from the heated wall to the bulk of the bed. The product was dry through the zone located between the heated wall and the vaporization front and a temperature gradient existed. The temperature and solvent content were assumed uniform and constant beyond the vaporization front. The concept of – the penetration – or the receding front model was to substitute the real continuous stirring periods by a fictitious sequence of rest steps, during which the bed was static, separated by an instantaneous perfect mixing of the bed. Good agreement between the simulated and experimental drying curves was observed, and the experimental drying times were well predicted by the improved model using six fitting parameters.

The penetration model has been long known and considered as the current industrial standard, but the main limitation is that the link to the kinematics of the granular flow is missing. The penetration model fails to consider the behavior of individual particles and hence does not describe inter-particle interactions.

3.2.2. Pore network technique

Pore network models, conventionally used to model drainage, are prevalent in the field of drying (Nowicki et al., 1992; Laurindo and Prat, 1998; Plourde and Prat, 2003; Segura and Toledo, 2005). The effect of structural parameters on drying kinetics can be investigated by studying the effective transport parameters and/or by using the structural information at the pore level to simulate the process. Hence, pore networks are used to describe the drying of porous media at the pore level. The network consists of regularly or randomly located pores that are interconnected by throats. To be characteristic of a real porous medium, the networks chosen should be large enough to have the same structural properties. Pore network simulations are qualitative in nature as the above mentioned prerequisites can only partly be achieved due to the lack of the experimental tools to analyze the structure of porous media at nano-scale.

Many researchers to date have simulated the drying process using networks without computing effective transport parameters and without variation of the pore structure. Most of these approaches assume isothermal conditions. Nowicki et al. (1992) obtained effective vapor diffusivity and relative liquid permeability as a function of degree of saturation. These properties were derived during drying of the pore network by using local vapor or liquid fluxes and corresponding gradients in vapor or capillary pressure. However, the impact of the network structure on drying behavior or on effective transport parameters was not investigated. Segura and Toledo (2005) computed diffusivity and permeability for pore saturations obtained from drying simulations. In their study, pore size distribution as well as throat shape were varied in order to study structural influences. Small range variations in pore size in the model made it difficult to draw conclusions.

Recently, in order to better understand the effect of pore size distribution on drying behavior, a one-dimensional capillary model was introduced by Metzger and Tsotsas (2005). Isothermal drying was modeled for a viscous liquid using plate and spherical porous objects. The pore space was represented by a bundle of cylindrical capillaries, set perpendicular to the product surface and connected without any lateral resistances. All relevant macroscopic properties of the porous medium were derived which were then employed in volume-averaged simulations to show the equivalence of continuous and discrete approaches. The validity of the model was limited due to its restriction to one dimension and the subsequent continuity of the liquid phase. The isothermal pore network model was used in parallel to study the dependence of drying kinetics on pore structure (Irawan et al., 2005; Metzger et al., 2005). The model assumes that the capillary forces are dominant. The network consisted of pore nodes lined by cylindrical throats of random radii which were selected corresponding to a pore size distribution. The throats were filled by liquid that can then evaporate through

one surface of the two- or three-dimensional network. The liquid phase typically becomes discontinuous during drying, splitting up into many clusters. The throats empty one by one within one cluster with decreasing radius because the liquid was always pumped to small throats. The drying rate was determined by vapor diffusion as computed from mass balances for all gas filled pores. They found that the drying simulations in two and three dimensions led to contradictory conclusions as in the 2D version, the capillary flow paths are easily cut off by emptying large throats suggesting that 3D modeling is crucial when structural influences are to be investigated. The main challenges associated with network modeling are that it does not account for all the transport effects and the network size should be representative or a number of small network simulations are required to get an average behavior.

3.2.3. Population balance models

In contrast to the traditional models, which compute only averages for all particles, population balance models include the evolution of properties that may differ from particle to particle, such as moisture content or temperature, and hence have the potential to be vastly superior and replace the existing models. Population balance models are used in fluidized bed operations, to describe the temporal change of the number density distribution of single particles with respect to different internal coordinates (velocity, etc.) and external coordinates (time and space). In the past, Burgschweiger (2000) suggested that these models are generally suited for continuously operated dryers. However, in a comparison with experimental data, it was found that such a model tends to underestimate the outlet moisture content. It seems clear that a better understanding of the process is needed, which will require much additional experimental data. Moreover, these models are limited to simple one-dimensional approaches as was shown in a study by Burgschweiger and Tsotsas (2002) where they considered the disperse solids as a single phase with average properties (i.e., particle size and moisture content). Population balances are models describing how the number of individuals in a population and their properties change with time and the conditions of growth.

3.2.4. Discrete element method (DEM)

The predominant method of discrete element simulation is based upon the pioneering work of Cundall and Strack (1979). DEM is a Lagrangian approach that tracks the positions, velocities, and accelerations of each particle. It explicitly considers inter-particle and particle-boundary interactions, providing an effective tool to solve the transient heat and mass transfer equations. A thorough description of the interaction laws can be found in McCarthy and Ottino (1998) and are therefore not reviewed here. The motion of individual particles is tracked by alternately computing forces between particles which are in contact and updating their positions accordingly. Contact forces are computed from the "overlap" of the particles and material properties describing stiffness and frictional slip. The forces on the particles apart from gravity typically are determined from contact mechanics considerations (Johnson, 1987). In their simplest form, these relations include normal, Hertzian, repulsion and some approximations of tangential friction (Mindlin, 1994). This approach, reviewed by several authors (Herrmann and Luding, 1998; Zhu et al., 2007), is valuable due to the high degree of detail describing the dynamic behavior of the particles. The particle positions and velocities can be used to calculate many particle-scale quantities of interest such as local temperatures and moisture content, as well as examine phenomena such as segregation or agglomeration. DEM not only offers a much more flexible approach with a direct relation between the material properties and the model parameters but also reduces the number of experiments and therefore facilitates better process understanding. Additionally, accurate predictions outside the range of available experiments as well as geometry effects such as the baffles design, etc., can be modeled precisely using DEM. These particulars are hard to address by continuum approaches.

Thermal particle dynamics (TPD) primarily introduced by Vargas and McCarthy (2000, 2001) incorporated both the contact mechanics and contact conductance theories to model the flow dynamics and heat conduction through the granular materials. The prime attribute of particle dynamics is that many concurrent two-body interactions may be used to simulate a many-body system (Cundall and Strack, 1979). This is because the time-step is chosen to be adequately small such that any displacement-induced disturbance does not propagate any further than that particle's immediate neighbors within one time-step. Similarly, contact mechanics for a two-body interaction are well understood (Johnson, 1987). TPD as first developed, included only the simplest well established conductance model (Fletcher, 1988; Sridhar and Yovanovich, 1994; Lambert and Fletcher, 1997), which initially assumed the impact of both interstitial fluid and thermal radiation were negligible. Even in its simplest form, TPD was capable of capturing particle-level temperature profiles not previously in literature, without using any adjustable parameters or comprehensive microstructural evidence. The authors concluded that the stress chains even in moderately imperfect crystals may cause damage in the way heat is transported by conduction.

Vargas and McCarthy (2002a) used a multi-scale modeling approach, thermal particle dynamics (TPD) — to examine heat conduction through a static, two-dimensional granular bed. Results of both experiments, and a microstructural based continuum model compare well with those obtained from TPD simulation. The technique was employed to simulate transient heat conduction in a two-dimensional packed bed and the results obtained were compared to both experiments and the theoretical predictions obtained from a fabric tensor-based effective conductivity expression (Jagota & Hui, 1990). Good qualitative and quantitative agreement for temperature profiles and predicted values of the effective thermal conductivity were obtained without requiring any freely adjustable parameters, despite the simplicity of TPD. Hence, TPD has shown to successfully predict the conductivity and transient temperature distribution of particle bed. Thermal particle dynamics method (TPD) was further extended by Vargas and McCarthy (2002b) to study heat conduction in granular media in the presence of stagnant interstitial fluids. The model not only clarifies fundamental issues in heat conduction in particulate materials, but also provides a valuable test bed for existing continuous theories.

Kwapinska et al. (2005) studied the heating of an agitated bed of mono-sized spheres in a rotating drum of constant wall temperature. They considered the limiting case where heat transfer was controlled by a wall-to-bed transfer coefficient. The temperature differences within the bed were negligible, and mixing does not play a role in overall heat transfer. Therefore, the particle-to-particle thermal resistance was set to a value close to zero. Results from the DEM showed that the evolution of the average bed temperature was found to coincide with the analytical solution. They demonstrated that DEM has the potential for realistically describing concurrent mixing and heat transfer patterns in the agitated beds. Kwapinska et al. (2008) investigated the ability of thermal DEM to provide information not accessible by the penetration model, like temperature distribution. The simulation results of thermal DEM were discussed and were in qualitative agreement with the experimental data and likewise with the classical penetration model (PM) for the following limiting cases: heat transfer controlled by a contact resistance at the wall of the drum; heat transfer to agitated beds with significant bed-side resistance; heat transfer to the stagnant bed. The authors suggested that thermal DEM has the potential to contribute significantly to process and product engineering in contact equipment.

Until recently, most of the DEM-based heat transfer work was either two-dimensional or in static granular beds. These simplifications have been made primarily because of the complexities of contact detection and the vast computational power required to model more complex systems (Ketterhagen et al., 2009). However, with the help of supercomputers and parallel computing techniques, it is not uncommon to use DEM to model bigger and complex systems with nonspherical particle shapes (Kodam et al., 2010) or interstitial fluid effects.

3.2.4.1. Interstitial fluid forces. Noncontact forces due to capillary cohesion or interactions may significantly affect the bulk behavior. The significance (Seville et al., 2000) and the application of such forces in DEM based models (Zhu et al., 2007) have been reviewed in the literature. The interstitial liquid is present in the form of pendular bridges. The forces exerted by the liquid bridge are capillary and viscous forces. The capillary force of a liquid bridge is calculated by Young's Laplace equation; however, this equation generally cannot be solved analytically. Thus, Fisher (1926) and thereafter Lian et al. (1996) assumed a torodial liquid bridge shape which allows for the estimation of the capillary force. Lian et al. (1996) showed that the error associated with this toroidal assumption is less than 10%. The capillary force, F_c, is calculated using the following relation: $F_c = 2\pi\gamma\rho_2(1 + H\rho_2)$, where γ is the surface tension, ρ_2 is the radius of the liquid bridge at the neck and H is the mean curvature. The approximate closed form solution is used to model the normal component of the viscous force of the liquid bridge between two spheres where the normal component is given by: $F_{vn} = 6\pi\eta R^* v_n R^*/S$, η is the viscosity, v_n is the relative normal velocity between two spheres, S is the separation distance and R^* is the reduced radius (Fisher, 1926). There is no rigorous analytical solution for the tangential component of the viscous force, but Goldman et al. (1967) derived the following asymptotic solution for the viscous force for sufficiently small separation distances: $F_{vt} = (8/15ln\ R/S + 0.9588)6\pi\eta R v_t$, where v_t is the relative normal velocity between two particles and R is the radius of the sphere (Adams and Edmonson, 1987). This approach has recently been used in DEM models to study the drying behavior in an agitated filter dryer (Chaudhuri et al., 2006; Sahni et al., 2011). Mikami et al. (1998) also suggested another approach to incorporate cohesive forces into DEM models. They developed regression expressions that provided an explicit calculation of the force as a function of the separation distance.

3.2.4.2. Prediction of attrition. Attrition being an inevitable phenomenon during the drying process can now be predicted using the discrete approaches. An attempt to predict the rate of attrition was recently made by Hare et al. (2011) to estimate the distribution of stresses and strains in a small-scale dryer using DEM in order to quantify the extent of attrition of Paracetamol. The data were fitted to the model developed by Neil and Bridgwater (1994). Acceptable quantitative agreement was found between the predictions and experimental results obtained for the attrition of Paracetamol in the small scale dryer. The predictions suggested that, for a given number of impeller rotations, the extent of breakage was independent of impeller speed in the ranges tested (20–78 rpm). The strain rate was highest at the outer radial positions in the vessel and decreased slightly at increased height. Moreover, over half of the attrition occurred in the bottom third of the bed with increased attrition at greater radial distances.

4. Concluding remarks

Drying is one of the most common unit operations in food, chemical, natural product and pharmaceuticals production. Work has ranged from fundamental studies using simple traditional approaches (e.g., LOD, KF, TGA) to gain insight into the underlying physics to use of PAT approaches (e.g., NIR, Raman) that attempt to elucidate the effects of particle properties and operational parameters on the process. The most favorable drying conditions often involve static drying coupled with intermittent agitation, or starting agitation at some specific level of LOD to avoid overdrying or damage to the crystals. Therefore, there is a need for stable and reliable models to quantify and predict the drying rates and drying times with useful accuracy. Moreover, knowledge of how particle properties affect the macroscopic properties is important for effective design, operation, and scale-up. The development of the models can complement our understanding of three-dimensional flow structures and they also have the capability to correlating the operating parameters, and particle properties with macroscopic properties like density, temperature, etc., thereby filling gaps in our knowledge of drying processes. In addition, modeling can yield information which is hard or sometimes impossible to ascertain from experiments.

Despite recent advances (Michaud et al., 2008a,; Murru et al., 2011) made toward comprehending drying phenomena, intricacies involved in the process not only due to the coupled nature of the process involving heat, mass and momentum transport (Whitaker, 1977) but also from their dependence on the material properties and drying conditions, do not allow quantitative predictions with extreme accuracy. Unlike traditional techniques, relevant quantities are modeled and measured locally and not in terms of averages. In this way, processes at the pore scale (for single particles) and for individual particles (for beds of particles) are not masked. Therefore, new insight into the drying processes at different scales may well be expected. Penetration models have been used because of their simplistic approach and have been modified over the years by various scientists. Additionally, thermal DEM models were limited to dry packed beds. Recently, studies have shown the emergence of DEM as a promising tool for complex system geometries, noncontact cohesive forces, and interstitial fluid effects.

Conflict of Interests

The authors report no conflict of interest.

Acknowledgement

We thank Dr. Michael Pikal to review the manuscript.

References

Abrahamsson, C., Johansson, J., Andersson-Engels, S., Svanberg, S., Folestad, S., 2005. Timeresolved NIR spectroscopy for quantitative analysis of intact pharmaceutical tablets. Anal. Chem. 77, 1055–1059.
Adams, M., Edmonson, B., 1987. Forces between particles in continuous and discrete liquid media. In: Briscoe, B.J., Adams, M.J. (Eds.), Tribology in Particle Technology. Adam Hilger, Bristol, pp. 154–172.
Arlabosse, P., Chitu, T., 2007. Identification of the limiting mechanism in contact drying of agitated sewage sludge. Drying Technol. 25, 557–567.
Baillon, B., 1996. Sechage sous vide micro-ondes combine de granules pharmaceutiques, Thesis, Universite de Pau et des Pays de l'Adour.
Bakeev, K.A., 2004. Near-infrared spectroscopy as a process analytical tool Part II: At-line and on-line applications and implementation strategies. Spectroscopy 19, 39–42.
Beer, T.D., Burggraeve, A., Fonteyne, M., Saerens, L., Remon, J.P., Vervaet, C., 2011. Near infrared and Raman spectroscopy for the in-process monitoring of pharmaceutical production processes. Int. J. Pharm. 417, 32–47.
Bellamy, L.J., Nordon, A., Littlejohn, D., 2008a. Real-time monitoring of powder mixing in a convective blender using non-invasive reflectance NIR spectrometry. Analyst 133, 58–64.
Bellamy, L.J., Nordon, A., Littlejohn, D., 2008b. Effects of particle size and cohesive properties on mixing studied by non-contact NIR. Int. J. Pharm. 361, 87–91.
Bemrose, C.R., Bridgwater, J., 1987. A review of attrition and attrition test methods. Powder Technol. 49, 97–126.
Burgschweiger, J., 2000. Modellierung des statischen und dynamischen Verhaltens von kontinuierlich betriebenen Wirbelschichttrocknern. Dissertation, Universität Magdeburg, VDI-Verlag, Reihe 3, No. 665.

Burgschweiger, J., Tsotsas, E., 2002. Experimental investigation and modelling of continuous fluidized bed drying under steady-state and dynamic conditions. Chem. Eng. Sci. 57, 5021–5038.
Burgbacher, J., Wiss, J., 2008. Industrial applications of online monitoring of drying processes of drug substances using NIR. Org. Process Res. Dev. 12, 235–242.
Carslaw, H.S., Jaeger, J.C., 1959. Conduction of Heat in Solids. Clarendon Press, Oxford.
Chao, R.S., Khanna, R.K., Lippincott, E.R., 1974. Theoretical and experimental resonance Raman intensities for the manganate ion. J. Raman Spectrosc. 3, 121–131.
Chaudhuri, B., Muzzio, F.J., Tomassone, M.S., 2006. Modeling of heat transfer in granular flow in rotating vessels. Chem. Eng. Sci. 61, 6348–6360.
Ciurczak, E.W., Torlini, R.P., Demkowcz, M.P., 1986. Determination of particle size of pharmaceutical raw materials using near infrared reflectance spectroscopy. Spectroscopy 1, 36–39.
Connors, K.A., 1988. The Karl Fisher titration of water. Drug Dev. Ind. Pharm. 14, 1891–1903.
Cundall, P.A., Strack, O.D.L., 1979. A discrete numerical model for granular assemblies. Geotechique 29, 47–55.
Deng, W.Y., Yan, J.H., Li, X.D., Wang, F., Lu, S.Y., Chi, Y., Cen, K.F., 2009. Measurement and simulation of the contact drying of sewage sludge in a Nara-type paddle dryer. Chem. Eng. Sci. 64, 5117–5124.
Farges, D., Hemati, M., Laguerie, C., Vachet, F., Rousseaux, P., 1995. A new approach to contact drying modeling. Drying Techol. 13, 1317–1329.
Findlay, W.P., Peck, G.R., Morris, K.R., 2005. Determination of fluidized bed granulation end point using near-infrared spectroscopy and phenomenological analysis. J. Pharm. Sci. 94, 604–612.
Fisher, R.A., 1926. On the capillary forces in an ideal soil; correction of formulae given by W.B. Haines. J. Agric. Sci. 16, 492–505.
Fletcher, L.S., 1988. Recent developments in contact conductance heat transfer. J. Heat Transf. 110, 1059–1071.
Forbert, R., Heimann, F., 1989. Vacuum contact drying of mechanically agitated, coarse, hygroscopic bulk material. Chem. Eng. Process. 26, 225–235.
Frake, P., Greenhalgh, D., Grierson, S.M., Hempenstall, J.M., Rudd, D.R., 1997. Process control and end-point determination of a fluid bed granulation by application of near infra-red spectroscopy. Int. J. Pharm. 151, 75–80.
Gardiner, D.J., Graves, P.R., Bowley, H.J., 1989. Practical Raman Spectroscopy. Springer-Verlag, New York.
Goldman, A.J., Cox, R.G., Brenner, H., 1967. Slow viscous motion of a sphere parallel to a plane wall-I motion through a quiescent fluid. Chem. Engng. Sci. 22, 637–651.
Gottfries, J., Depui, H., Fransson, M., Jongeneelen, M., Josefson, M., Langkilde, F.W., Witte, D.T., 1996. Vibrational spectroscopy for the assessment of active substance in metoprolol tablets: a comparison between transmission and diffuse reflectance near-infrared spectrometry. J. Pharm. Biomed. Anal. 14, 1495–1503.
Green, R.L., Thurau, G., Pixley, N.C., Mateos, A., Reed, R.A., Higgins, J.P., 2005. In-line monitoring of moisture content in fluid bed dryers using near-IR spectroscopy with consideration of sampling effects on method accuracy. Anal. Chem. 77, 4515–4522.
Grigull, U., Sandner, H., 1984. In: Munz Brienza, B. (Ed.), Heat Conduction. Hemisphere Publishing Corporation, United States of America.
Guidance for Industry, 2004. PAT — A Framework for Innovative Pharmaceutical Development, Manufacturing, and Quality Assurance, September 2004. http://www.fda.gov/cvm/guidance/published.html.
Hamilton, P., Littlejohn, D., Nordon, A., Sefcik, J., Slavin, P., Dallin, P., Andrews, J., 2011. Studies of particle drying using non-invasive Raman spectrometry and particle size analysis. Analyst 136, 2168–2174.
Hare, C., Ghadiri, M., Dennehy, R., 2011. Prediction of attrition in agitated particle beds. Chem. Eng. Sci. 66, 4757–4770.
Heimann, F., Schlünder, E.U., 1988. Vacuum contact drying of mechanically agitated granulate beds wetted with a binary mixture. Chem. Eng. Proc. 24, 75–91.
Herrmann, H.J., Luding, S., 1998. Modeling granular media on the computer. Continuum Mech. Therm. 10, 189–231.
Hu, Y.R., Wikström, H., Byrn, S.R., Taylor, L.S., 2006. Analysis of the effect of particle size on polymorphic quantitation by Raman spectroscopy. Appl. Spectrosc. 60, 977–984.
Irawan, A., Metzger, T., Tsotsas, E., 2005. Pore network modelling of drying: combination with a boundary layer model to capture the first drying period. Proc. 7th WCCE, Glasgow, United Kingdom.
Jagota, A., Hui, C.Y., 1990. The effective thermal conductivity of a packing of spheres. J. Appl. Mech. 57, 789–791.
Johnson, K.L., 1987. Contact Mechanics. Cambridge University Press, Cambridge.
Keey, R.B., 1972. Drying: Principles and Practice. Pergamon, New York.
Keey, R.B., 1992. Drying of Loose and Particulate Materials. Hemisphere Publishing, New York.
Ketterhagen, W.R., Am Ende, M.T., Hancock, B.C., 2009. Process modeling in the pharmaceutical industry using the discrete element method. J. Pharm. Sci. 98, 442–470.
Kimball, G., 2001. Direct vs. irect drying: optimizing the process. Chem. Eng., 74–81.
Kodam, M., Bharadwaj, R., Curtis, J., Hancock, B., Wassgren, C., 2010. Cylindrical object contact detection for use in discrete element method simulations, Part II-Experimental validation. Chem. Eng. Sci. 65, 5863–5871.
Kogermann, K., Aaltonen, J., Strachan, C.J., Pollanen, K., Veski, P., Heinamaki, J., Yliruusi, J., Rantanen, J., 2007. Qualitative in situ analysis of multiple solid-state forms using spectroscopy and partial least squares discriminant modeling. J. Pharm. Sci. 96, 1802–1820.
Kogermann, K., 2008. Understanding solid-state transformations during dehydration: new insights using vibrational spectroscopy and multivariate modelling. DOSIS 24, 150.
Kohout, M., Collier, A.P., Stepanek, F., 2004. Vacuum contact drying of crystals: multi-scale modelling and experiments. In: Barbosa-Povoa, A., Matos, H. (Eds.), ESCAPE-14. Elsevier Science, Amsterdam, pp. 1075–1080.
Kohout, M., Collier, A.P., Stepanek, F., 2005. Vacuum contact drying kinetics: an experimental parametric study. Drying Technol. 23, 1825–1839.
Kohout, M., Collier, A.P., Stepanek, F., 2006. Mathematical modelling of solvent drying from a static particle bed. Chem. Eng. Sci. 61, 3674–3685.
Kohout, M., Collier, A.P., Stepanek, F., 2007. Multi-scale analysis of vacuum contact drying. Drying Technol. 25, 1265–1273.
Kosek, J., Stepanek, F., Marek, M., 2005. Modelling of transport and transformation processes in porous and multi-phase bodies. Adv. Chem. Eng. 30, 137–203.
Kwapinska, M., Saage, G., Tsotsas, E., 2005. On the way from penetration models to discrete element simulations of contact dryers. In: XI Polish Drying Symposium, Poznan, Poland.
Kwapinska, M., Saage, G., Tsotsas, E., 2008. Continuous versus discrete modelling of heat transfer to agitated beds. Powder Technol. 181, 331–342.
Lachman, L., Lieberman, H.A., Kanig, J.L., 1990. The Theory and Practice of Industrial Pharmacy, third ed. Vargiese Publishing House.
Lambert, M.A., Fletcher, L.S., 1997. Review of models for thermal contact conductance of metals. J. Thermophys. Heat Transf. 11, 129–140.
Laurindo, J.B., Prat, M., 1998. Numerical and experimental network study of evaporation in capillary porous media. Chem. Eng. Sci. 53, 2257–2269.
Lekhal, A., Girard, K.P., Brown, M.A., Kiang, S., Glasser, B.J., Khinast, J.G., 2003. Impact of agitated drying on crystal morphology: KCl–water system. Powder Technol. 132, 119–130.
Lekhal, A., Girard, K.P., Brown, M.A., Kiang, S., Khinast, J.G., Glasser, B.J., 2004. The effect of agitated drying on the morphology of L-threonine (needle-like) crystals. Int. J. Pharm. 270, 263–277.
Lian, G., Adams, M., Thornton, C., 1996. Elastohyrdodynamic collisions of solid spheres. J. Fluid Mech. 311, 141–152.
Lodder, R.A., Hieftje, G.M., 1988. Analysis of intact tablets by near-infrared reflectance spectrometry. Appl. Spectrosc. 42, 556–558.
Long, D.A., 1977. Raman Spectroscopy. McGraw-Hill International, New York.
Luypaert, J., Massart, D.L., Heyden, V.Y., 2007. Near-infrared spectroscopy applications in pharmaceutical analysis. Talanta 72, 865–883.
Malczewski, J., Kaczmarek, W., 1989. Vacuum contact drying of seeds. Drying Technol. Int. J. 7, 59–69.
Malhotra, K., Mujumdar, A.S., 1987. Immersed surface heat transfer in vibrated fluidized beds. Ind. Eng. Res. 26, 1983–1992.
Malhotra, K., 1989. Particle flow and contact heat tranfer characteristics of stirred granular beds. Ph.D. thesis, McGill University, Canada.
Malhotra, K., Okazaki, M., 1992. Contact drying in mechanically agitated granular beds: A review of fundamentals. In: Mujumdar, A.S. (ed.). In Advances in Drying, Vol. 5, Hemisphere.
Mazzarotta, B., Cave, S.D., Bonifazi, G., 1996. Influence of time on crystal attrition in a stirred vessel. AIChE 42, 3554–3558.
McCarthy, J.J., Ottino, J.M., 1998. Particle dynamics simulation: a hybrid technique applied to granular mixing. Powder Technol. 97, 91–99.
McCormick, P.Y., 1988. The key to drying of solids. Chem. Eng. (Aug. 15), 113–122.
McCreery, R.L., 2000. Raman spectroscopy for chemical analysis. New York, Wiley-Interscience, A John Wiley & Sons, Inc., Publication.
Metzger, T., Irawan, A., Tsotsas, E., 2005. Discrete modeling of drying kinetics of porous media. In: Proc. 3rd Nordic Drying Conference, Karlstad, Sweden.
Metzger, T., Tsotsas, E., 2005. Influence of pore size distribution on drying kinetics: a simple capillary model. Drying Technol. 23, 1797–1809.
Michaud, A., Peczalski, R., Andrieu, J., 2007. Experimental study and modeling of crystalline powders vacuum contact drying with intermittent stirring. Drying Technol. 25, 1163–1173.
Michaud, A., Peczalski, R., Andrieu, J., 2008a. Modeling of vacuum contact drying of crystalline powders packed beds. Chem. Eng. Proc. Process Intensificat. 47, 722–730.
Michaud, A., Peczalski, R., Andrieu, J., 2008b. Optimization of crystalline powders vacuum contact drying with intermittent stirring. Chem. Eng. Res. Design 86, 606–611.
Mikami, T., Kamiya, H., Horio, M., 1998. Numerical simulation of cohesive powder behavior in a fluidized bed. Chem. Eng. Sci. 53, 1927–1940.
Mindlin, R.D., 1994. Compliance of Elastic Bodies in Contact. J. Appl. Mech. 16, 333.
Mollekopf, N., Schlünder, E.U., 1982. Contact drying of granulated product under vacuum. In: Ashworth, J.C. (ed.). In Proc. 3rd Int. Drying Symp., vol. 2. Drying Research Ltd., UK, p. 502.
Moyne, C., 1987. Tranferts couples chaleur-masse loris du sechage: prise en compte du mouvement de la phase gazeuse, Thesis, Institut National polytechnique de Lorraine.
Mujumdar, A.S., 2007. Handbook of Industrial Drying, third ed. Taylor and Francis, Philadelphia.
Murru, M., Giorgio, G., Montomoli, S., Ricard, F., Stepanek, F., 2011. Model-based scale-up of vacuum contact drying of pharmaceutical compounds. Chem. Eng. Sci. 66, 5045–5054.
Nastaj, J.F., 1994. Vacuum contact drying of selected biotechnological products. Drying Technol. 12, 1145–1166.
Neil, A.U., Bridgwater, J., 1994. Attrition of particulate solids under shear. Powder Technol. 80, 207.
Nowicki, S.C., Davis, H.T., Scriven, L.E., 1992. Microscopic determination of transport parameters in drying porous media. Drying Technol. 10, 925–946.
Parris, J., Airiau, C., Escott, R., Rydzak, J., Crocombe, R., 2005. Monitoring API drying operations with NIR. Spectroscopy 20, 34–42.

Pelletier, M.J., 2003. Quantitative analysis using Raman spectrometry. Appl. Spectrosc. 57, 20A–42A.
Plourde, F., Prat, M., 2003. Pore network simulations of drying of capillary porous media. Influence of thermal gradients. Int. J. Heat Mass Transfer 46, 1293–1307.
Rantanen, J., Lehtola, S., Rämet, P., Mannermaa, J.P., Yliruusi, J., 1998. On-line monitoring of moisture content in an instrumented fluidized bed granulator with a multichannel NIR moisture sensor. Powder Technol. 99, 163–170.
Rantanen, J., Yliruusi, J., 1998. Determination of particle size in a fluidized bed granulator with a near infrared set-up. Pharm. Pharmacol. Commun. 4, 73–75.
Räsänen, E., Rantanen, J., Jørgensen, A.C., Karjalainen, M., Paakkari, T., Yliruusi, J., 2001. Novel identification of pseudopolymorphic changes of theophylline during wet granulation using near infrared spectroscopy. J. Pharm. Sci. 90, 389–396.
Reich, G., 2005. Near-infrared spectroscopy and imaging: basic principles and pharmaceutical applications. Adv. Drug Deliv. Rev. 57, 1109–1143.
Root, W.L., 1983. Indirect drying of solids. Chem. Eng., 52–63.
Sahni, E., Hallisey, J., Morgan, B., Strong, J., Chaudhuri, B., 2011.Quantifying drying performance of Filter Dryer: Experiments and Simulations, Advanced Powder Technology, http://dx.doi.org/10.1016/j.apt.2011.03.002.
Schlünder, E.U., 1980. Contact drying of particulate material under vacuum. In: Mujumdar, A.S. (ed.). Drying '80. Hemisphere, Washington, D.C, p.184.
Schlünder, E.U., Mollekopf, N., 1984. Vacuum contact drying of free flowing mechanically agitated particulate material. Chem. Eng. Process. 18, 93–111.
Segura, L.A., Toledo, P.G., 2005. Pore-level modeling of isothermal drying of pore networks. Effects of gravity and pore shape and size distributions. Chem. Eng. J. 111, 237–252.
Seville, J.P.K., Willett, C.D., Knight, P.C., 2000. Interparticle forces in fluidisation: A review. Powder Technol. 113, 261–268.
Shering, P., 2005. Engineering a system to enable spectroscopy in a filter dryer, Process Spectroscopy, SPECTROSCOPY EUROPE, 17, AstraZeneca Engineering Technology, Alderley House, Alderley Park, Macclesfield 6, pp. 30–31.
Siesler, H.W., 2002. Near-infrared Spectroscopy: Principles, Instruments, Applications. John Wiley & Sons, March 20.
Skansi, D., Tomas, S., Pudic, I., Arapovic, A., 1997. The influence of pressure and temperature on the kinetics of vacuum drying of ketoprofen. Drying Technol. 15, 1617–1631.
Slangen, H.J.M., 2000. The need for fundamental research on drying as perceived by the European chemical industry. Drying Technol. 18, 1601–1604.
Sridhar, M.R., Yovanovich, M.M., 1994. Review of elastic and plastic contact conductance models: Comparison with experiment. J. Thermophys. Heat Transfer 8, 633–640.
Stephenson, G.A., Forbes, R.A., Reutzel-Edens, S.M., 2001. Characterization of the solid state: quantitative issues. Adv. Drug Deliv. Rev. 48, 67–90.
Suzuki, K., Ikeda, M., Esaka, M., Kubota, K. 1985. Characteristics of vibrofluidized bed freeze drying. In: Toei, R., Mujumdar, A.S. (eds.), Drying '85. Hemisphere, Washington, D.C., p. 254.
Sztabert, Z.T., 1989. Size selection of vacuum contact dryer with mechanically mixed particulate material. Drying Technol. Int. J. 7, 71–85.
Thurner, F., 1993. Contact drying in the chemical industry. Chem. Eng., 20–22.
Tsotsas, E., 1985. Über den Einfluß der Dispersität und der Hygroskopizität auf den Trocknungsverlauf bei der Vakuum-Kontakttrocknung rieselfähiger Trocknungsgüter, Dissertation, Universität Karlsruhe.
Tsotsas, E., Schlünder, E.U., 1986. Vacuum contact drying of free flowing mechanically agitated particulate multigranular packing. Chem. Eng. Process. 20, 339–349.
Tsotsas, E., Schlünder, E.U., 1987. Vacuum contact drying of mechanically agitated beds: the influence of hygroscopic behaviour on the drying rate curve. Chem. Eng. Process. 21, 199–208.
Uhl, V.W., Root, W.L. 1962. Indirect drying in agitated units. Chem. Eng. Progr, 37.
Vargas, W.L., McCarthy, J.J., 2000. Unsteady heat conduction in granular materials. Mater. Res. Soc. Symp.– Proc. 627, BB391–BB396.
Vargas, W.L., McCarthy, J.J., 2001. Heat conduction in granular materials. AIChEJ 47, 1052–1059.
Vargas, W.L., McCarthy, J.J., 2002a. Stress effects on the conductivity of particulate beds. Chem. Eng. Sci. 57, 3119–3131.
Vargas, W.L., McCarthy, J.J., 2002b. Conductivity of granular media with stagnant interstitial fluids via thermal particle dynamics simulation. Int. J. Heat Mass Transf. 45, 4847–4856.
Wang, H.L., Mann, C.K., Vickers, T.J., 2002. Effect of powder properties on the intensity of Raman scattering by crystalline solids. Appl. Spectrosc. 56, 1538–1544.
Wei, C.K., Davis, H.T., Davis, E.A., Gordon, J., 1987. Evaporation from porous media: a capillary model of a penetrating front. Chem. Eng. Commun. 56, 269–284.
Whitaker, S., 1977. Simultaneous heat, mass and momentum transfer in porous media–a theory of drying. Adv. Heat Transf. 13, 119–203.
Whitaker, S., 1980. Heat and mass transfer in porous granular media. In: Mujumdar, A.S. (ed.). Advances in Drying. Hemisphere, Washington, D.C., pp. 23.
Workman, J., Weyer, L., 2008. Practical guide to interpretive near-infrared spectroscopy.
Zhou, G.X., Ge, Z., Dorwart, J., Izzo, B., Kukura, J., Bicker, G., Wyvratt, J., 2003. Determination and differentiation of surface and bound water in drug substances by near infrared spectroscopy. J. Pharm. Sci. 92, 1058–1065.
Zhu, H.P., Zhou, Z.Y., Yang, R.Y., Yu, A.B., 2007. Discrete particle simulation of particulate systems: Theoretical developments. Chem. Eng. Sci. 62, 3378–3396.